Prospective longitudinal study of immune checkpoint molecule (ICM) expression in immune cell subsets during curative conventional therapy of head and neck squamous cell carcinoma (HNSCC)

Adrian Witzleben, Adrian Fehn, Ayla Grages, Jasmin Ezić, Sandra S. Jeske, Lisa K. Puntigam, Cornelia Brunner, Johann M. Kraus, Hans A. Kestler, Johannes Doescher, Matthias Brand, Marie Nicole Theodoraki, Christian H. Ottensmeier, Thomas K. Hoffmann, Patrick J. Schuler, Simon Laban

TUMOR IMMUNOLOGY AND MICROENVIRONMENT

IJC
International Journal of Cancer

Prospective longitudinal study of immune checkpoint molecule (ICM) expression in immune cell subsets during curative conventional therapy of head and neck squamous cell carcinoma (HNSCC)

Adrian von Witzleben[1,2,3] | Adrian Fehn[1] | Ayla Grages[1] | Jasmin Ezić[1] |
Sandra S. Jeske[1] | Lisa K. Puntigam[1] | Cornelia Brunner[1] | Johann M. Kraus[4] |
Hans A. Kestler[4] | Johannes Doescher[1] | Matthias Brand[1] |
Marie-Nicole Theodoraki[1] | Christian H. Ottensmeier[2,3] |
Thomas K. Hoffmann[1] | Patrick J. Schuler[1] | Simon Laban[1]

[1]Department of Otorhinolaryngology and Head & Neck Surgery, University Medical Center Ulm, Head and Neck Cancer Center of the Comprehensive Cancer Center Ulm, Ulm, Germany

[2]University of Southampton, Faculty of Medicine, Cancer Sciences Unit, Southampton, UK

[3]Southampton University Hospitals NHS foundation Trust, Southampton, UK

[4]Ulm University, Institute for Medical Systems Biology, Ulm, Germany

Correspondence
Simon Laban, Department of Otorhinolaryngology and Head & Neck Surgery, University Medical Center Ulm, Head and Neck Cancer Center of the Comprehensive Cancer Center Ulm, Frauensteige 12, 89075 Ulm, Germany.
Email: simon.laban@gmail.com

Funding information
Deutsche Forschungsgemeinschaft, Grant/Award Numbers: 288342734 (GRK-2254), 416718265; Ulm University, Faculty of Medicine, Grant/Award Number: Clinician Scientist Programme

Abstract

Programmed-death-1 (PD1) antibodies are approved for recurrent and metastatic head and neck squamous cell carcinoma. Multiple drugs targeting costimulatory and coinhibitory immune checkpoint molecules (ICM) have been discovered. However, it remains unknown how these ICM are affected by curative conventional therapy on different immune cell subsets during the course of treatment. In the prospective non-interventional clinical study titled "Immune Response Evaluation to Curative conventional Therapy" (NCT03053661), 22 patients were prospectively enrolled. Blood samples were drawn at defined time points throughout curative conventional treatment and follow-up. Immune cells (IC) from the different time points were assessed by multicolor flow cytometry. The following ICM were measured by flow cytometry: PD1, CTLA4, BTLA, CD137, CD27, GITR, OX40, LAG3 and TIM3. Dynamics of ICM expression were assessed using nonparametric paired samples tests. Significant changes were noted for PD1, BTLA and CD27 on multiple IC types during or after radiotherapy. Nonsignificant trends for increased expression of OX40 and GITR from baseline until the end of RT were observed on CD4 T cells and CD4$^+$ CD39$^+$ T cells. In patients with samples at recurrence of disease, a nonsignificant increase of TIM3 and LAG3 positive CD4$^+$ CD39$^+$ T cells was evident, accompanied by an increase of double positive cells for TIM3/LAG3. Potential future targets to be combined with RT in the conventional treatment and anti-PD1/PD-L

Abbreviations: ADCC, antibody-dependent cellular cytotoxicity; BTLA, B and T lymphocyte attenuator; CRT, definitive chemoradiotherapy; CTLA4, cytotoxic T lymphocyte antigen 4; GITR, glucocorticoid-induced TNFR family related protein; HNSCC, head and neck squamous cell carcinoma; HPV, human papillomavirus; IC, immune cell; ICM, immune checkpoint molecules; IRECT, Prospective non-interventional clinical study titled "Immune Response Evaluation to Curative conventional Therapy"; LAG3, lymphocyte activation gene 3; PBMC, peripheral blood mononuclear cells; PD-L1, programmed-death-ligand-1; PD1, programmed-death-1; R/M, recurrent or metastatic; RT, adjuvant (chemo)radiotherapy; TIM3, T-cell immunoglobulin and mucin-domain containing-3; TNFR, tumor necrosis factor receptors; TP, time point; WBC, white blood cell count.

Adrian von Witzleben and Adrian Fehn contributed equally and share first authorship.

- -

could be BTLA agonists, or agonistic antibodies to costimulatory ICM like CD137, OX40 or GITR. The combination of cetuximab with CD27 agonistic antibodies enhancing ADCC or the targeting of TIM3/LAG3 may be another promising strategy.

KEYWORDS

cancer immunotherapy, curative treatment, head and neck squamous cell carcinoma, immune checkpoint

1 | BACKGROUND

Globally, head and neck squamous cell carcinoma (HNSCC) is diagnosed in almost 900 000 cases annually resulting in approximately 450 000 cancer deaths per year.[1] Internationally, the conventional curative treatment of locoregionally advanced HNSCC is either surgery followed by risk-adapted adjuvant (chemo)radiotherapy (RT) or definitive chemoradiotherapy (CRT).[2] The importance of immunotherapy primarily the modulation of immune checkpoint molecules (ICM) is continuously increasing. Inhibitory antibodies to the ICM programmed-death-1 (PD1) have been established as standard of care for platinum-naïve recurrent or metastatic (R/M) HNSCC as a monotherapy or in combination with cisplatin and 5-fluoruracil[3] and as a monotherapy for platinum-refractory R/M HNSCC.[4,5] Considering the poor prognosis of locoregionally advanced HNSCC, there is a large potential for improvement by integrating immunotherapy into the curative treatment of locoregionally advanced HNSCC. In ongoing clinical trials, antibodies inhibiting the PD1/programmed-death-ligand-1 (PD-L1) axis are empirically combined with conventional treatment in the curative setting.[6-8] Multiple potentially targetable ICM have been identified. Among others, these include costimulatory ICM like CD137, OX40, glucocorticoid-induced tumor necrosis factor receptors (TNFR) family related protein (GITR) and CD27 or coinhibitory ICM like PD1, cytotoxic T lymphocyte antigen 4 (CTLA4), B and T lymphocyte attenuator (BTLA), lymphocyte activation gene 3 (LAG3) or T-cell immunoglobulin and mucin-domain containing-3 (TIM3). To date, the impact of curative conventional treatment on the expression of ICM on immune cells (IC) has not been systematically investigated in HNSCC. Thus, a rationale for the timing of treatment with different ICM modulators within the course of conventional treatment and potential combination partners is lacking.

Within the prospective noninterventional clinical study titled "Immune Response Evaluation to Curative conventional Therapy (IRECT)" (NCT03053661), systematic immune monitoring was performed longitudinally during conventional treatment of locoregionally advanced HNSCC.[9] Here, we present flow cytometry data assessing nine ICM on peripheral T and B cells from patients harvested during the course of curative treatment and follow-up.

What's new?

While standard therapy for HNSCC generally includes surgery plus radiotherapy, immunotherapy for HNSCC is increasing in importance. Here, the authors provide the first prospective clinical study systematically analyzing the expression of 9 different immune checkpoint molecules over multiple time points during conventional therapy and follow up. Radiotherapy, but not surgery, profoundly impacts the expression of immune modulating molecules. Expression of PD1, BTLA, and CD27 changed significantly after radiotherapy, findings which could help improve treatment decisions. BTLA+ cells, for example, declined gradually following radiotherapy, suggesting that targeting BTLA agonists could be a promising strategy.

Curative conventional Therapy (IRECT)" (NCT03053661) between August 2013 and April 2015. The study was performed after approval by the local ethics committee of Ulm University (222/13). Patients with stage III/IVa HNSCC (AJCC classification version 7) who were candidates for curative conventional treatment were included after informed consent. HNSCC was confirmed histopathologically. Human papillomavirus (HPV) status was determined for all oropharyngeal primary tumors by multiplex HPV-DNA PCR (GP5+/GP6+ primers) followed by Sanger sequencing for HPV typing as previously described[10] and p16INK4a immunohistochemistry (Clone 1D7D2, Invitrogen) was performed using a DAKO autostainer. Individual treatment recommendations were based on clinical disease and patient features as determined in a weekly interdisciplinary team discussion at the Comprehensive Cancer Center Ulm according to current international treatment guidelines and in consideration of patient preferences. Patients received either a primary surgical treatment (Arm A: surgery followed by risk-adapted adjuvant treatment, n = 18) or a primary radiotherapeutic treatment (Arm B: primary CRT; n = 4). The treatment recommendation was independent of the noninterventional study participation.

2 | METHODS

2.1 | Patients

Twenty-two patients were enrolled into the prospective non-interventional clinical study titled "Immune Response Evaluation to

2.2 | Blood Samples

Fifty milliliters of whole blood (citrate-buffered) were prospectively collected at baseline and at protocol-specified time points (TPs) during curative conventional treatment and during posttreatment follow-up as indicated in Figure 1 (Arm A: 8 samples [TPs 1A, 1B, 4, 6, 7, 8,
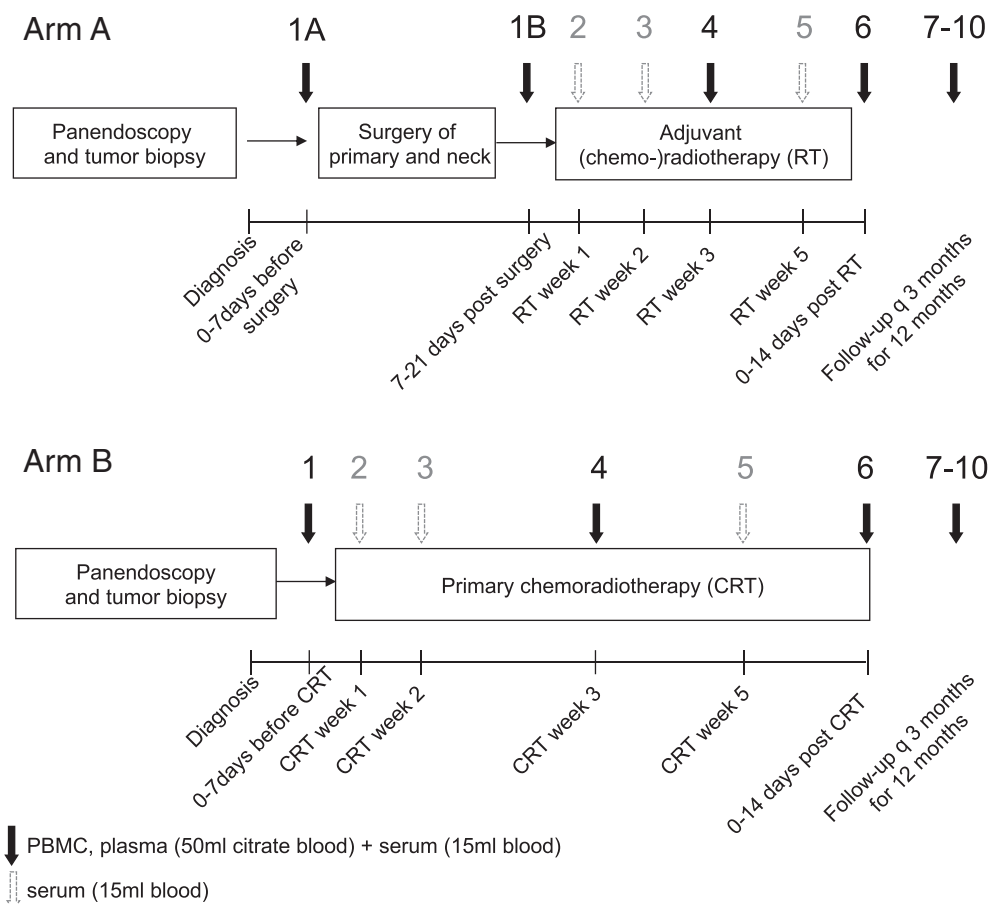
FIGURE 1 Schematic study overview. Patients were allocated to Arm A (surgical treatment + risk-adapted adjuvant radiotherapy, RT ± chemotherapy) or Arm B (chemoradiotherapy, CRT) based on the interdisciplinary tumor board recommendation and patient preferences. Sampling was performed as defined in the protocol at specified parallel time points in Arm A and B. The full arrow represents a 50 mL whole blood sample (citrate-buffered) and a 15 mL sample (serum tubes). Open arrows (gray) represent a 15 mL sample for serum only (serum tubes). Only the whole blood samples containing peripheral blood mononuclear cells (PBMC) were used in this part of the study (black arrows). The baseline sample (Arm A: Sample 1A, Arm B: Sample 1) was taken prior to treatment initiation. In Arm A, an additional sample was taken during post-surgery recovery phase (Sample 1B). Samples were also taken mid-RT/mid CRT (Sample 4) and at the end of RT/CRT (Sample 6) as well as every 3 months during post-treatment follow-up for 12 months (Sample 7-10)

9, 10]; Arm B: 7 samples [TPs 1, 4, 6, 7, 8, 9, 10]). An additional sample was collected at the time of recurrence if applicable. Healthy control blood samples were taken after informed consent and treated as described for the patient samples.

Peripheral blood mononuclear cells (PBMC) were isolated by density centrifugation from whole blood using Leucosep tubes (Greiner bio-one, Frickenhausen, Deutschland) per manufacturer's instruction. 5×10^6 PBMC were aliquoted and frozen in RPMI1640 medium with fetal bovine serum and 10% dimethylsulfoxide and stored in liquid nitrogen until use.

Additionally, a differential white blood cell count (WBC) had been planned at every TP per protocol, but differential WBC samples were only available for 75 of the 172 planned samples.

2.3 | Flow cytometry

PBMC were stained for multicolor flow cytometry. Three flow cytometry panels with four backbone markers (CD8: FITC [clone SK1,

eBioscience, Waltham, MA], CD4: Alexa Fluor 700 [clone OKT4, eBioscience], CD39: PE Cy7 [clone eBioA1, eBioscience], CD19: APC Fire [clone HIB19, BioLegend, London, UK]) were designed. CD8 T cells were defined as $CD8^+/CD4^-$, CD4 T cells were defined as $CD4^+/CD8^-$. A subgroup of CD4 T cells was gated as $CD4^+/CD39^+$. CD39 is expressed in 60% of FOXP3+ regulatory T cells and a positive linear correlation between CD39 and FoxP3 has been reported.[11] $CD4^+/CD39^+$ T cells are in our study assumed to be an antigen-experienced type of Treg. $CD19^+/CD4^-$ cells were defined as CD19 B cells.

Each flow cytometry panel consisted of three ICM added to the backbone markers. Panel 1 consisted of PD1 (PE, clone eBioJ1 05, eBioscience), CTLA4 (PE Cy5, clone BNI3, BD Bioscience, San Jose, CA) and BTLA (Brilliant Violet 421, MIH26, BioLegend). Panel 2 consisted of CD137 (PE, clone 4B4, eBioscience), CD27 (PE Cy5, clone 0323, eBioscience), GITR (Brilliant Violet 421, clone 108-17, BioLegend) and panel 3 of OX40 (PE Cy5, clone Ber-ACT35, BioLegend), LAG3 (PE, clone 3DS22 3H eBioscience) and TIM3 (Pacific Blue, F38-2E2, BioLegend). Stained samples were measured on a Beckman Coulter Gallios

flow cytometer. Cytometric data were gated and analyzed using Kaluza software by Beckman Coulter as displayed in Supplementary Figure S1. The four backbone marker gates were defined as CD8 T cells (CD8$^+$/CD4$^-$), CD4 T cells (CD4$^+$/CD8$^-$), CD4$^+$/CD39$^+$ T cells (CD4$^+$/CD8$^-$/CD39$^+$), and CD19 B cells (CD19$^+$/CD4$^-$).

ICM positive gates were defined in healthy samples after stimulation with Interleukin 2 (IL-2, 320 IU/mL) 48 hours before measurement (Supplementary Figure S2).

2.4 | Statistics

Since backbone markers were available from all three ICM panels, mean values of relative IC numbers were calculated and compared between TPs by Kruskal-Wallis test.

Wilcoxon signed rank tests for paired samples were performed to compare relative IC fractions and ICM expression of the nine ICM at the respective TP to the individual patient's baseline using SPSS statistics version 25. To correct for the large number of hypotheses tested due to the high number of sample TPs, cellular subsets (CD8, CD4, CD19, CD4/CD39) and ICM analyzed, a false discovery rate approach was used. The two-stage linear step-up procedure of Benjamini, Krieger and Yekutieli was used for correction of multiple testing (Q = 5%) using GraphPad Prism (version 8.4.2). Data were graphed using GraphPad Prism (version 8.4.2). Venn diagrams of median single, double and triple expression among the respective ICM flow cytometry panels were graphed using eulerAPE as previously described.[12]

3 | RESULTS

Among the 22 patients who were enrolled in the study, 18 patients were treated by surgery followed by risk-based RT (2 patients declined adjuvant treatment and 3 had no indication for RT by pTNM). Four patients received definitive primary CRT. Additional patient characteristics are displayed in Table 1.

Of 172 samples planned per protocol, 134 samples were available for analysis (77.9%; median sample number: 7; mean sample number:

TABLE 1 Patient characteristics

			n	%
Primary site	Oral cavity		5	23%
	Oropharynx		12	55%
	Hypopharynx		3	14%
	Larynx		2	9%
	Total		22	100%
Sex	Male		19	86%
	Female		3	14%
Age	mean (range)		62.4 (50-79)	n.a.
Smoking	Pack years: median (range)		40 (0-80)	n.a.
	Never		3	14%
	Former		11	50%
	Current		8	36%
Alcohol	Never		2	9%
	Moderately		4	18%
	Daily		11	50%
	Missing		5	23%
HPV-status (DNA/p16)	Negative		14	64%
	Positive		7	32%
	Missing		1	5%
Treatment	Primary surgery + risk adapted adjuvant RT (Arm A)	Surgery only[a]	5	23%
		Surgery + adj. RT	8	36%
		Surgery + adj. CRT	5	23%
		Total Arm A	18	82%
	Primary CRT (Arm B)		4	18%
PBMC samples	<5 samples available		4	18%
	≥5 samples available		18	82%

Abbreviations: CRT, chemoradiotherapy; HPV, human papillomavirus; RT, radiotherapy.

[a]Three patients had no indication for adj. RT based on pTNM. Two declined adjuvant RT.

6.1). Eighteen patients (82%) provided ≥5 samples. Reasons for missing samples were treatment complications (n = 3 patients), screening failure due to an unreported prior malignancy (n = 1 patient), decline of indicated adjuvant treatment (n = 2 patients, both recurred), withdrawal from longitudinal sampling during the course of treatment (n = 3), stage I/II disease after surgical staging voiding the need for adjuvant treatment (n = 2).

3.1 | Radiotherapy not surgery has a prolonged impact on the IC composition

IC numbers are visualized in Supplementary Figure S3. Mean relative IC numbers changed significantly during treatment for CD8+ (P = .017) and CD4+ T cells (P < .0001), CD19+ B cells (P < .0001), but not CD4+/CD39+ T cells (P = .924). CD8+ T cell fractions decreased continuously from the time of surgery until the end of RT (Sample 6). Paired samples tests revealed a significant decrease at TP 6. Three months after RT (Sample 7), CD8+ T cell fractions had returned to baseline and remained stable. CD4+ T cells exhibited a significant decrease within the postsurgical window (sample 1B) and decreased further until TP 6. Three months after RT (Sample 7), CD4+ T cell fractions began to slowly increase until 12 months after the end of treatment but remained significantly lower than the individual baseline. For CD4+/CD39+ T cells, no significant changes of relative numbers were noted throughout the treatment. B cells, determined by expression of CD19, also decreased significantly beginning mid-RT (Sample 4) and remained significantly lower until 3 months after end of treatment (Sample 7). Six months after RT B-cell fractions had returned to baseline levels.
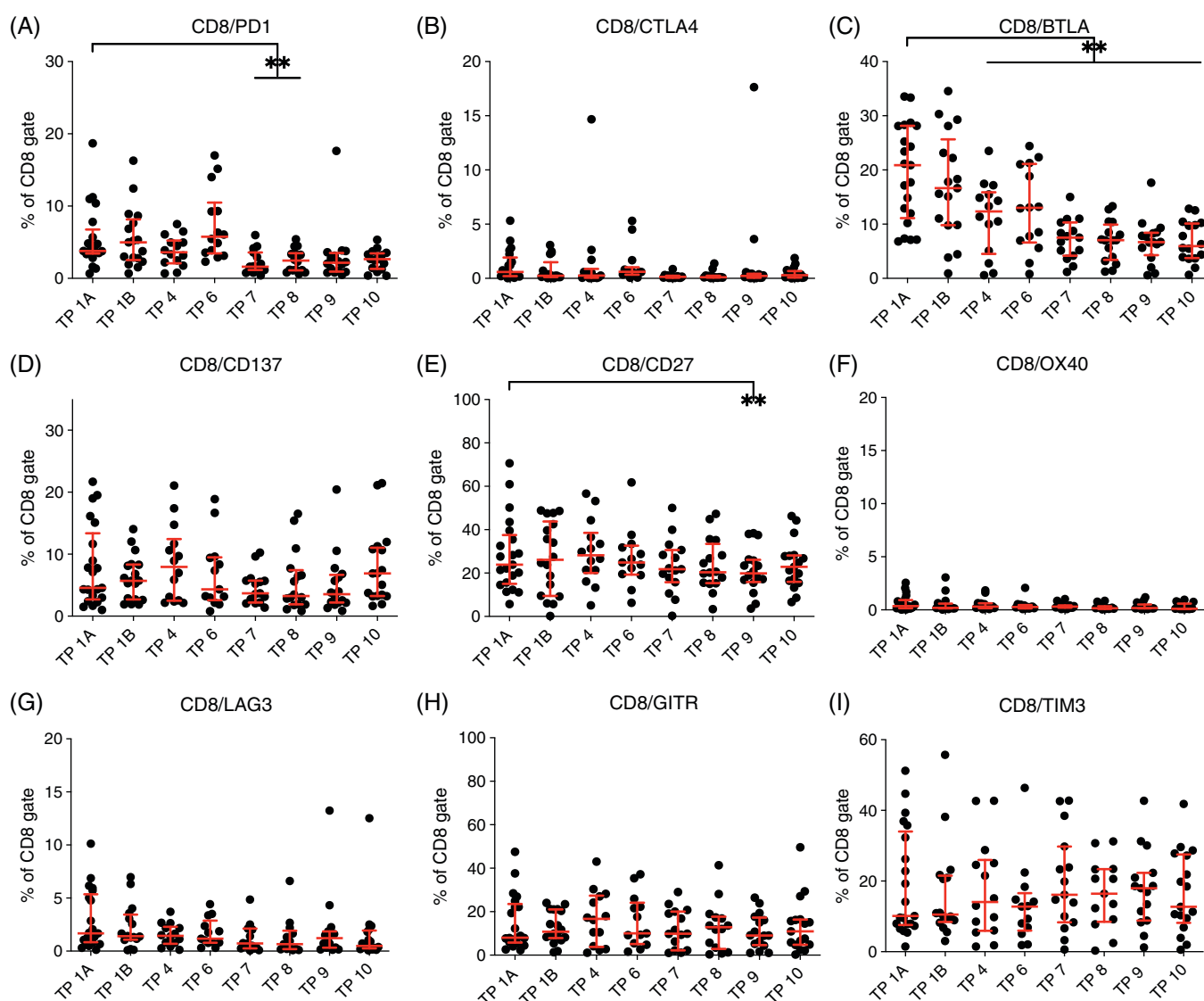

FIGURE 2 Immune-checkpoint molecule (ICM) expression on CD8 T cells. The fraction of ICM positive CD8 T cells in percent is displayed on the y-axis. On the x-axis, the respective sampling time point (TP) is indicated. All available data points per time point are displayed in a scatter plot with the median and interquartile range in red. Significant differences compared to the baseline sample based on nonparametric paired samples tests (Wilcoxon signed rank test) are marked with asterisks (*P < .05, **P < .01)

Due to the low number of available differential WBC at baseline (n = 3), the absolute numbers of CD8$^+$ T cells, CD4$^+$ T cells, CD4$^+$/CD39$^+$ T cells and CD19$^+$ B cells could not be compared longitudinally to the individual baseline sample. Instead, based on the available samples, absolute numbers of CD8$^+$ T cells, CD4$^+$ T cells and CD4$^+$/CD39$^+$ T cells were compared over the sample period as a whole by Kruskal-Wallis test and did not change significantly (P > .4). However, the absolute CD19$^+$ B-cell numbers changed significantly throughout the course of treatment (Kruskal-Wallis, P = .0002) mirroring the curve of relative B-cell fractions.

ICM expression did not change significantly from baseline (Sample 1A) in the postsurgical period (Sample 1B) in patients recruited in Arm A. In contrast, significant changes were observed during and after radiotherapy.

The fraction of ICM positive CD8$^+$ T cells is shown in Figure 2. On CD8$^+$ T cells, the expression of PD1 increased at the end of RT (Sample 6) as compared to baseline, but this increase was not statistically significant in paired samples tests. However, PD1 expression declined significantly after the end of RT. Compared to the baseline, the percentage of PD1 positive cells among CD8$^+$ T cells was significantly lower at 3 and 6 months after the end of radiotherapy (Samples 7 and 8). The proportion of BTLA$^+$CD8$^+$ T cells declined gradually after surgery, reaching a significantly lower BTLA expression mid-RT (Sample 4) and remaining significantly lower until 12 months after the end of treatment (Sample 10). The fraction of CD27$^+$ CD8$^+$ T cells was significantly lower 9 months after end of treatment (Sample 9). The proportion of CTLA4 expression, CD137, OX40, LAG3, GITR and TIM3 did not change significantly on CD8$^+$ T cells over the course of
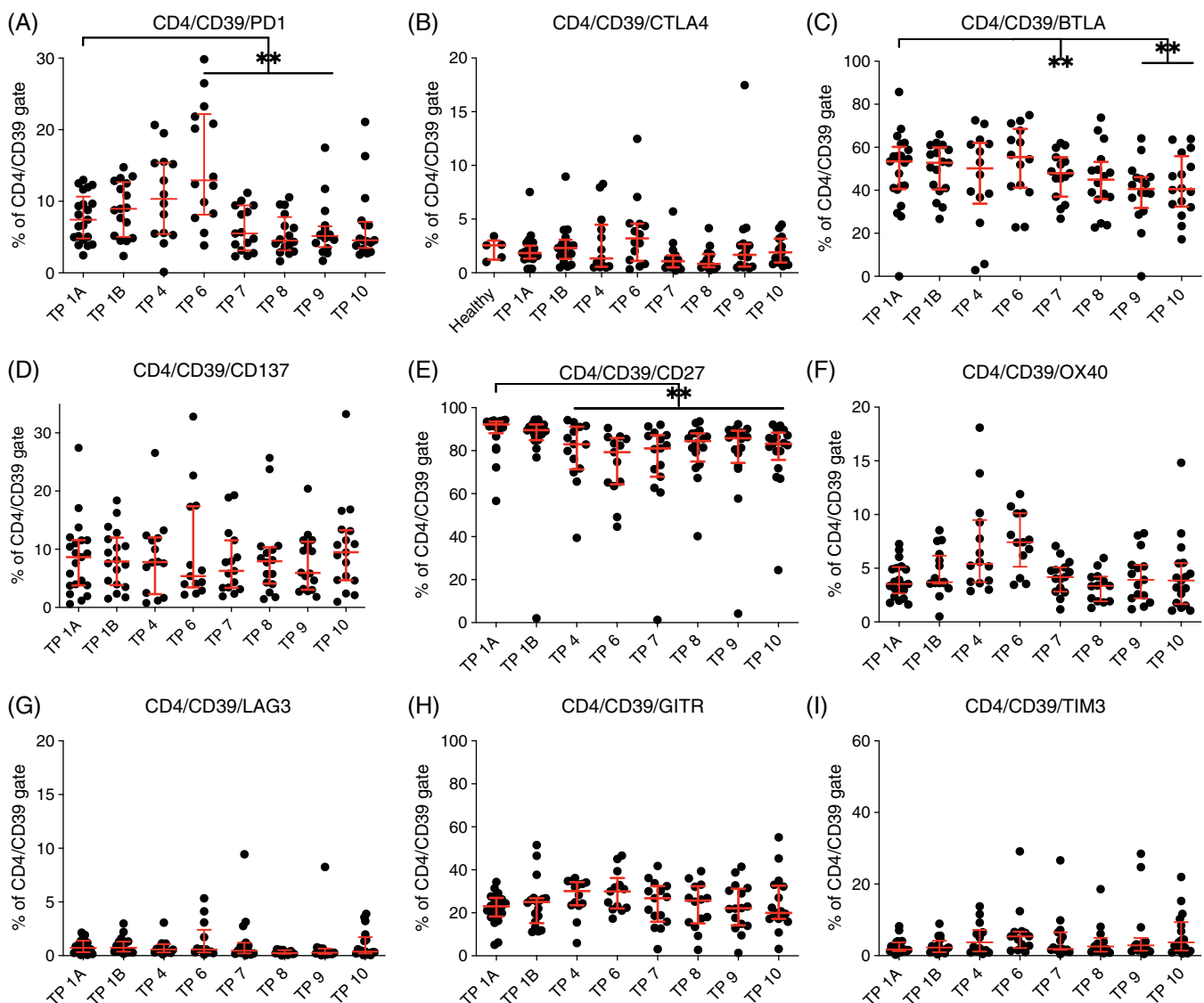

FIGURE 3 Immune-checkpoint molecule (ICM) expression on CD4/CD39 T cells. The fraction of ICM positive CD4/CD39 T cells in percent is displayed on the y-axis. On the x-axis, the respective sampling time point (TP) is indicated. All available data points per time point are displayed in a scatter plot with the median and interquartile range in red. Significant differences compared to the baseline sample based on nonparametric paired samples tests (Wilcoxon signed rank test) are marked with asterisks (*P < .05, **P < .01, ***P < .001)

treatment. However, a considerable proportion of cells was TIM3 positive at baseline (mean = 19.2%), but expression levels showed a wide variation (95% CI: 12.3-26.0). The high variability of TIM3 expression was also observed for all other TPs in CD8$^+$ T cells.

The percentage of ICM positive CD4$^+$ T cells is shown in Supplementary Figure S4. The fraction of PD1 CD4$^+$ positive cells increased significantly at the end of RT (Sample 6) but returned to baseline thereafter. The contribution of BTLA$^+$CD4$^+$ T cells decreased gradually over the course of treatment. From 3 months after RT (Sample 7) until the end of the evaluation period (Sample 10), the fraction of BTLA expressing cells was significantly lower than at baseline. CD27 expression rate declined during treatment and remained significantly lower than baseline from mid-RT until the end of the evaluation period. OX40 and GITR expression increased from baseline until the end of RT, but the increase did not remain significant after correction

for multiple testing. All other ICM fractions did not change significantly during treatment.

The percentage of ICM positive CD4$^+$/CD39$^+$ T cells, as a subpopulation of the CD4$^+$ T cells, is graphed in Figure 3. CD4$^+$/CD39$^+$ T cells were considered as a fraction of antigen-experienced regulatory T cells. In this cell population, the fraction of PD1 positive cells also increased during RT, reaching significantly higher levels at the end of radiotherapy (Sample 6). Subsequently, PD1 positive cell fraction dropped significantly below the baseline and remained this way until 9 months after the end of treatment. BTLA expressing cells were significantly less frequent immediately after RT and 9-12 months after the end of RT. In parallel to CD4$^+$ T cells, CD27 expression rate on CD4$^+$/CD39$^+$ T cells also declined during treatment and remained significantly lower than baseline from mid-RT until the end of the evaluation period. More pronounced than in CD4$^+$ T cells, OX40 and GITR expression increased
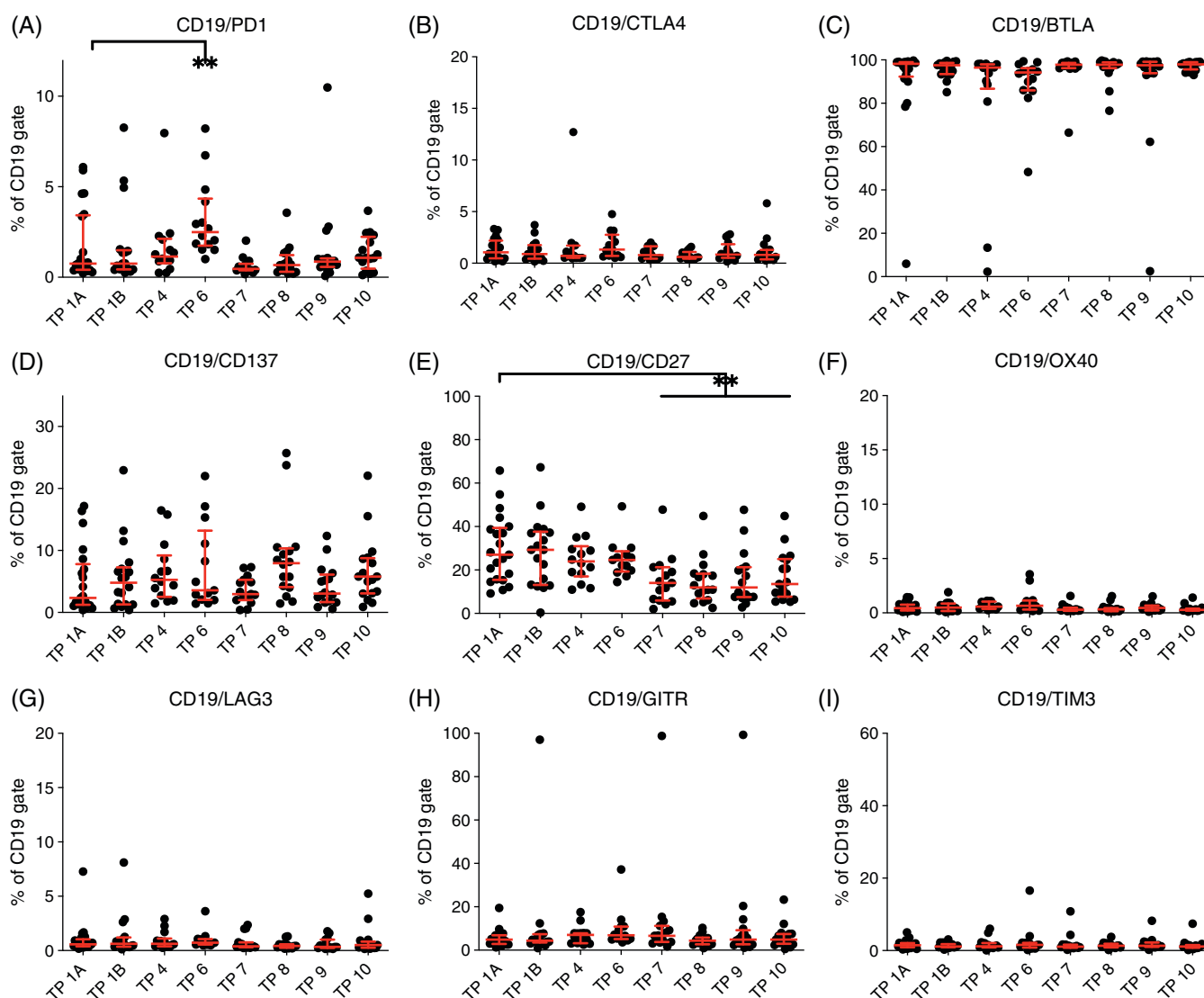

FIGURE 4 Immune-checkpoint molecule (ICM) expression on CD19 B cells. The fraction of ICM positive CD19 B cells in percent is displayed on the y-axis. On the x-axis, the respective sampling time point (TP) is indicated. All available data points per time point are displayed in a scatter plot with the median and interquartile range in red. Significant differences compared to the baseline sample based on nonparametric paired samples tests (Wilcoxon signed rank test) are marked with asterisks (*P < .05, **P < .01)

from baseline until the end of RT on CD4$^+$/CD39$^+$ T cells, but the increase did not remain significant after correction for multiple testing.

The percentage of ICM positive B cells is graphed in Figure 4. The rate of PD1 expression on B cells increased during radiotherapy reaching significantly higher expression rates after RT (Sample 6). As in CD4$^+$ T cells, the fraction of CD27 positive cells continuously declined during RT, resulting in significantly lower fractions of CD27 positive B cells from 3 months after RT until the end of the evaluation period. The positivity rate of other ICM did not change significantly during treatment.

3.2 | Changes in ICM expression at the time of treatment failure

During follow-up (mean follow-up time: 60.6 months), 8/22 patients suffered from recurrent disease (regional = 1, locoregional = 2, second head and neck primary = 3, distant = 1, local/regional and distant = 1). All of those patients were HPV-negative. Recurrent disease was treated with curative intent in five patients and palliatively in the remaining three patients. A PBMC sample from the time of recurrence

was available for 6/8 recurrent patients. The individual courses of ICM in CD4$^+$/CD39$^+$ T cells of the six patients with recurrent disease and available samples are provided in Figure 5A-L. At the time of the diagnosis of recurrent disease or after this diagnosis, we observed an increase of TIM3 and LAG3 positive CD4$^+$/CD39$^+$ T cells. Based on the proportion of positive cells normalized to the baseline value, the increase in TIM3 and LAG3 positive CD4$^+$/CD39$^+$ T cells was up to 11-fold. In paired samples tests, this difference did not reach significance.

Next, the number of double and triple positive CD4$^+$/CD39$^+$ T cells in the different ICM panels were assessed (Figure 6). The median positive percentage including the interquartile range is graphed as Venn diagrams for baseline (TP 1) and the time of recurrence in Figure 6. The results were statistically compared between baseline and recurrence samples for single, double and triple positive cell fractions using Wilcoxon signed rank test for related samples and corrected for multiple testing (Q = 5%). None of the comparisons reached statistical significance, but trends to increased coexpression were observed at the time of recurrent disease for each ICM triplets (Panel 1: PD1, CTLA4, BTLA; Panel 2: CD137, CD27, GITR; and Panel 3: LAG3, OX40, TIM3).
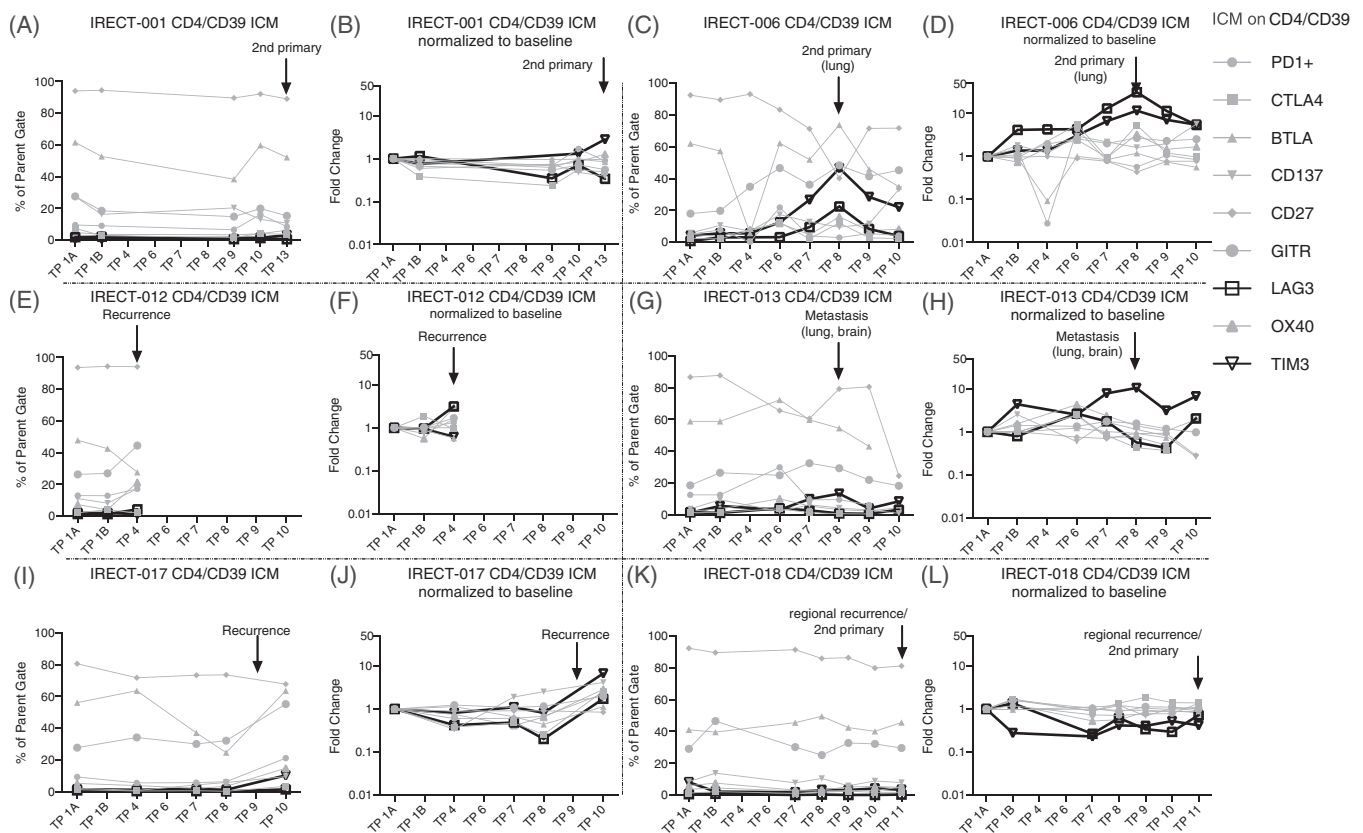

FIGURE 5 Immune-checkpoint molecule (ICM) expression on CD4/CD39 T cells of recurrent disease patients. Visualization of patient-specific longitudinal data for all ICM are displayed for six patients with recurrent disease at some point during follow-up. Panels A, C, E, G, I and K display the positive fraction of ICM positive CD4/CD39 T cells for the respective ICM in percent on the y-axis. Panels B, D, F, H, J and L show the same values after normalization to the respective baseline to improve the visualization of ICM dynamics. The ICM LAG3 and TIM3 are highlighted in bold print. On the x-axis, the respective sampling time point (TP) is indicated
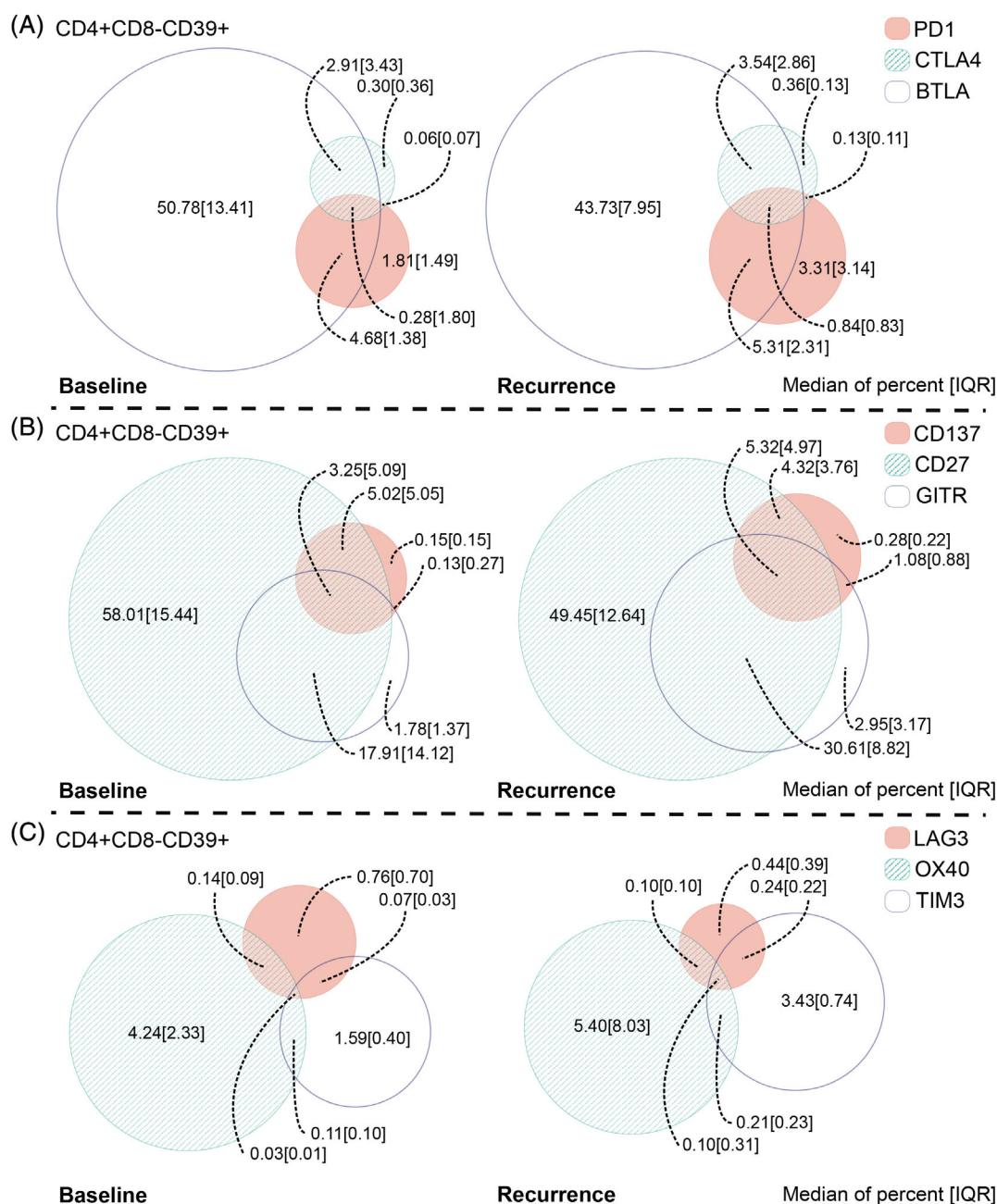
FIGURE 6 Venn diagrams of single, double and triple expression of immune-checkpoint molecules (ICM). Venn diagrams are shown for patients with recurrent disease only (n = 6). The median percentage and interquartile range (IQR) of single-, double- and triple-positive cells is indicated in the respective circles and overlapping areas at baseline and the time of recurrence

4 | DISCUSSION

We provide the first prospective clinical study systematically analyzing the expression of nine targetable ICM in IC subsets at multiple TPs during conventional treatment and follow-up of HNSCC. The ICM assessed in this project can be grouped into costimulatory molecules/members of the TNFR family like CD137, OX40, GITR and CD27 and coinhibitory ICM like PD1, CTLA4, BTLA, LAG3 and TIM3.

CD137, also called 4-1BB, has its expression peak 48 hours after lymphocyte activation and binds to CD137 ligand on antigen

presenting cells (APC).[13] OX40 is also expressed on activated T cells especially CD28+ T cells. After binding of OX40 to OX40L expressed on activated APCs, the T-cell activation is reinforced.[13] The GITR ligand is also expressed on APCs and can activate either GITR+ T cells but also have costimulatory effect on GITR+ CD4+ CD25+ Tregs.[13] While the first interaction between T cells and APC would lead to T-cell activation, the latter would results in T-cell suppression through TREGs. CD27 binds to CD70 or antibodies which can enhance CD4+ and CD8+ T-cell activation. Additionally, CD27 plays a role in B-cell interaction and germinal center formation.[13] PD1, CTLA4, BTLA,

LAG3 and TIM3 are T-cell exhaustion markers and can get upregulated in case of chronic infection or cancer. While PD1 is binding to its ligand PD-L1, CTLA4 interacts with CD80/CD86 and BTLA with HVEM. LAG3 binds to MHC molecules, Galactin-3 and FGL-1. TIM3 interacts with CEACAM-1 on APCs and Galactin-9 as well as HMGB-1 on tumor cells.[14]

All patients were treated in accordance with international treatment guidelines and blood samples were drawn prospectively at defined TPs during the course of treatment and follow-up. In another published study, patient samples were collected at baseline, immediately after the end of radiotherapy and 1 month later,[15] but no additional samples were collected during radiotherapy, follow-up nor at the time of recurrent disease. Also, the group studied only the ICM PD1 and CTLA4. In accordance with our findings, an increased fraction of PD1 positive CD4$^+$ T cells was described. In contrast to our findings, the group observed an increase in the fraction of CTLA4$^+$ CD4$^+$ T cells, whereas no such dynamics were observed in our cohort.

The majority of patients in our study was treated with a primary surgical approach followed by risk-adapted adjuvant RT/CRT which is the preferred standard of care at most centers in Germany.[16,17] In the study by Balazs et al, only patients treated with definitive chemoradiation without prior surgery were included. The removal of the primary tumor and the draining lymph nodes is the accepted surgical standard for locoregionally advanced HNSCC. Although surgery is a traditional pillar of the treatment for cancer, our understanding of the impact of surgery on the immune system is limited. In our study, surgery had a minor impact on the relative number of most IC subsets except for CD4$^+$ T cells which decreased significantly after surgery. This decline continued during radiotherapy reaching a minimum of the CD4$^+$ T-cell fraction immediately after the end of radiotherapy. This decline in the periphery may be caused by a recruitment of CD4$^+$ T cells to the surgical wound in the former tumor area. The continued decrease until end of (C)RT may also be caused by the locoregional induction of cell death and inflammation caused by the adjuvant radiation treatment.

The expression rate of the nine ICM evaluated did not change significantly postsurgery. The sampling window after surgery was 7 to 21 days after surgery to allow for unimpaired surgical recovery. This rather wide window may have diluted immediate effects after surgery.

In contrast to these minor effects of cancer surgery, radiotherapy—whether adjuvant or definitive—had a much higher impact resulting in a relative decrease of CD8$^+$ and CD4$^+$ T cells as well as B-cell numbers whereas CD4$^+$/CD39$^+$ T cells were not affected. The majority of changes in the relative number of positive ICM also occurred in temporal association with radiotherapy. Whereas PD1 positive cells increased significantly in CD4$^+$ T cells, CD19$^+$ B cells and CD4$^+$/CD39$^+$ T cells after RT, a nonsignificant increase was observed already during RT in all IC types. At 3 to 6 months after RT, PD1 positive cells were significantly lower than at baseline in CD8$^+$ T cells and CD4$^+$/CD39$^+$ T cells. A similar finding of increased PD1 expression has been previously described after whole body irradiation in mice resulting in impaired T-cell metabolism upon

T-cell receptor activation.[18] These findings are clinically important since in clinical trials, inhibitory antibodies of the PD1/PD-L1 axis are being investigated in combination with RT alone[19] or CRT as a definitive[20-22] or adjuvant treatment[23] (radiotherapy anti-PD1/PD-L1 combinations were reviewed previously[8]). Nevertheless, the timing of PD1/PD-L1 blockade in combination with radiotherapy remains under debate and tested empirically.[8] Our data would suggest that anti-PD1/PD-L1 may have the highest impact if initiated in the middle of or immediately after RT. However, it remains unclear whether the expanding PD1 positive cells are stimulated antigen-specific ICs expanded due to pro-inflammatory stimuli of radiotherapy or rather immunosuppressive ICs counteracting to such inflammatory stimuli.[8,24]

Another ICM showing dynamic changes in all T-cell subsets evaluated, but not in B cells is BTLA—a coinhibitory ICM negatively regulating T cells.[25] BTLA positive cells are continuously decreasing during treatment in CD8$^+$ and CD4$^+$ T cells and to a much lesser extent in CD4$^+$/CD39$^+$ T cells, whereas BTLA expression in B cells was very high throughout the whole study phase. In ovarian cancer patients, high BTLA expression has been associated with poor survival.[26] BTLA inhibition has demonstrated enhanced anti-cancer effects in an ovarian cancer mouse model when combined with chemotherapy by reducing regulatory CD19$^+$ B cells.[26] CD8$^+$ T cells coexpressing BTLA have previously also been associated with better responses to autologous adoptive cell therapy in melanoma.[27] Since BTLA is predominantly expressed on B cells, but also on a relevant fraction of T cells, BTLA antibodies may synergize with anti-PD1/PD-L1 antibodies.

CD27 positive cells declined among the CD4$^+$ T cells, the CD39$^+$CD4 fraction but also among CD19$^+$ B cells after radiotherapy reaching a minimum immediately after RT but remaining significantly lower than at baseline throughout the evaluation period. In a lymphoma mouse model, CD27 antibodies synergized with anti-CD20 antibody treatment by the stimulation of T cells and NK cells to release myeloid attracting cytokines. This resulted in increased myeloid cell infiltration and activation enhancing the elimination of CD20 antibody opsonized lymphoma cells.[28] Whether CD27 agonistic antibodies are useful combination partners in HNSCC remains unclear. Since cetuximab, a monoclonal EGFR antibody is known to elicit antibody-dependent cellular cytotoxicity (ADCC),[29,30] similar effects may be possible in HNSCC when combining CD27 agonists with cetuximab.

No significant changes during and after treatment were observed for other costimulatory ICM. There were trends observed for an increase in CD27 and CD137 expression on CD8 T$^+$ cells and increasing OX40 and GITR expression in CD4$^+$/CD39$^+$ T cells during radiotherapy. These results did not reach statistical significance which may be due to the limited patient number in our study. Subtle changes in the expression of costimulatory ICM which did not reach significance levels might still be relevant, considering that effects in the tumor may be diluted in the blood compartment. A combination of agonistic costimulatory antibodies against CD137, OX40 or GITR with radiotherapy may synergize with anti-PD1/PD-L1 inhibition by expanding antigen-specific activated ICs. The expression of ICM from the tumor

necrosis factor receptor (TNFR) family signaling pathways such as CD137, OX40 and GITR on regulatory T cells seems to be important for the maintenance of effector Treg cell populations,[24] which may explain the increase of OX40 and GITR we observed on CD4+ CD39+ T cells during radiotherapy.

Another interesting aspect was the increase in TIM3 and LAG3 positive cells in CD4/CD39 T cells at the time of recurrent disease diagnosis. Our observation of increased double positive TIM3/LAG3 positive cells in CD4/CD39 T cells at the time of recurrence may indicate an important role of these ICM in the development of recurrent disease and may at the same time represent a druggable target for such patients. TIM3 has been described as a marker of highly dysfunctional T cells in cancer and chronic viral infection.[31,32] TIM3 among CD39 and other markers has been described as one of the distinct features of tumor infiltrating lymphocytes in recurrent glioblastoma.[32] In another study in acute myeloid leukemia, bone marrow aspirates were assessed for different ICM. TIM3 or LAG3 coexpression with PD1 was found frequently in T cells of AML patients. However, the increased coexpression was found primarily in CD8 cells and not in CD4/CD39 T cells.[33] In HNSCC, the coexpression of LAG3 and TIM3 with other coinhibitory receptors such as PD1 and CTLA4 was found in a subset of terminally differentiated CD8 T cells and in CD4 T cells may prevent differentiation into T follicular helper cells.[24]

CD39 has been shown to be expressed in the majority of FoxP3+ T cells and a positive linear correlation between CD39 and FoxP3 is reported.[11] However, those CD39+ Tregs are reported to act highly immune suppressive through breaking down ATP or ADP to immunosuppressive adenosine using their ectonucleoside triphosphate diphosphohydrolase-1 function.[34] The CD39 expression is reported to be associated with a more stable Treg type.[35] Additionally, it is also reported that CD39 expression depends on patients age and diseases.[11,36] Summarized, CD39 detects a subgroup of stable FoxP3+ T cells, which are shown to include the most suppressing cell type and assumed to be an antigen-specific and -experienced type of Tregs. However, not all CD4+ T cells that are CD39+ are regulatory T cells. CD4+ CD39+ CD45RO+ FoxP3– T cells present a type of effector memory T cells producing IFNγ and IL17A.[37] The coexpression of CD39 and CD103 on CD8+ T cells has been reported to identify cancer-specific immunity.[38] Another recently published study also described that antigen-specific ICs are highly enriched among the CD39+ fraction of CD4+ or CD8+ T cells.[39] These findings may allow a different perspective on our data in the CD4+ CD39+ cells. Unfortunately, the omission of additional markers to discriminate further between Treg and antigen-specific effector memory cells in our panel is a relevant shortcoming.

We selected CD39 as a Treg marker due to the limitations of other surface markers such as CD25 or intracellular markers such as FoxP3. These markers can be found on other cells (activated effector T cells) or used to detect a heterogeneous group of Tregs including both highly and minimally suppressing cells, respectively.[40] Of note, a combination of different markers would have been a good approach for detecting Tregs properly. Although as the result of few flow cytometry channels, we concluded to use only one authenticating surface marker knowing the limitations not to use more marker to characterize Tregs in terms of feasibility. Consequently and to prevent promiscuity, we decided not to use the term Treg in our article, as for a correct characterization more essential markers (CD3, CD4, CD25, FoxP3 and CD127) should have been used.[41] However, we expect that the CD4/CD39 T cells present in the majority highly suppressive Treg, especially those coexpressing LAG3 and TIM3 at the time of recurrent disease. This notion is supported by increased levels of mainly inhibitory cytokines in the peripheral blood (IRECT-001: IL10, IRECT-006 and IRECT-018: IL4) at the time of recurrent disease (data not shown). In some patients, a sharp increase of High Mobility Group Box 1 (IRECT-001, -013, -017, -018), known to act immunosuppressively on T cells,[42,43] was measured around the time of disease recurrence as previously published.[9] A recently published study using single cell RNA sequencing of peripheral and intratumoral lymphocytes indicates that the coexpression of LAG3 and TIM3 inhibits CD4 T cells to develop into T follicular helper cells and instead may promote development into a suppressive phenotype.[24]

Strengths of the study are the longitudinal sampling enabling paired samples tests, the predefined sampling TPs and the precisely defined patient group. A similar immune monitoring of HNSCC patients during conventional therapy has not been published previously.

Nevertheless, there are certain limitations to our study. Patient recruitment was planned for 18 months and it was estimated that at least 50 patients could be recruited during this time. Due to the longitudinal sampling with the necessity of multiple additional visits, patient recruitment was much lower than expected. Additionally, due to treatment related complications, discrepancies between clinical and pathological staging voiding the indication for adjuvant RT and patient withdrawals, several important samples could not be obtained. The limited patient number and missing samples impede the power of identifying relevant dynamics statistically.

There is a known discrepancy between tumor infiltrating lymphocytes and peripheral blood lymphocytes. Tumor-infiltrating lymphocytes contain more antigen-specific effector memory cells and regulatory ICs than peripheral cells restricting the abstraction of analyses from peripheral blood.[44-46] However, there is recirculation of T cells, B cells and Tregs from the tumor tissue into the lymph nodes and the blood. Therefore, detecting ICM on peripheral IC enables indirect assessment of differences in between patients and TPs. Since this was a longitudinal study, the repeated harvesting of tumor infiltrating lymphocytes, especially in surgically resected patients, would not have been feasible.

A caveat of the flow data is that we have not provided absolute numbers for the different cell population which can be skewed by treatment or disease dependent lymphocyte count changes. We focused on lymphocyte subsets and did not include markers for nonlymphocytic myeloid or NK cells which preclude any statements hitherto.

Another methodologic limitation is the design of three different ICM panels for flow cytometry limiting the analysis of ICM coexpressing cells from different panels.

This limitation may have been avoided using mass cytometry (CyTOF) instead of flow cytometry or a cytometer with more lasers to include more markers, but access to such equipment was not possible.

In conclusion, these data provide a comprehensive analysis of the dynamics of ICM expression during the conventional treatment of HNSCC. The radiotherapy effects on periphery lymphocytes and their expression of multiple ICM were strong and long-lasting. Our findings underpin the importance of investigation of ICM on ICs and could be fundamental for further functional assessment of those subsets. On a clinical perspective, BTLA agonists, or agonistic antibodies to costimulatory ICM like CD137, OX40 or GITR could become potential future targets to be combined with RT in the conventional treatment or anti-PD1/PD-L1 therapy. The combination of cetuximab with CD27 agonistic antibodies enhancing ADCC or the targeting of TIM3/LAG3 may be another promising strategy.

CONFLICT OF INTEREST

Simon Laban: Advisory Boards: Merck Sharp & Dohme (MSD), Bristol Myers Squibb (BMS), Astra Zeneca (AZ). Honoraria: MSD, BMS, AZ, Merck Serono. Johannes Döscher: Advisory Boards: Merck Serono, MSD. Honoraria: Merck Serono. Thomas K. Hoffmann: Advisory Boards: MSD, BMS. Honoraria: MSD, BMS, Merck Serono. Patrick Schuler: Advisory Boards: BMS, MSD. All the other authors declared no potential conflicts of interest.
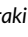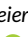
DATA AVAILABILITY STATEMENT

Data can be obtained from the authors upon reasonable request.

ETHICS STATEMENT

The study was performed after approval by the local ethics committee of Ulm University (222/13). Written informed consent was obtained from all patients. Trial registration number: NCT03053661.

ORCID

Adrian von Witzleben https://orcid.org/0000-0001-6766-4758
Cornelia Brunner https://orcid.org/0000-0002-6456-5508
Hans A. Kestler https://orcid.org/0000-0002-4759-5254
Johannes Doescher https://orcid.org/0000-0001-8997-8387
Marie-Nicole Theodoraki https://orcid.org/0000-0002-5491-1593
Christian H. Ottensmeier https://orcid.org/0000-0003-3619-1657
Thomas K. Hoffmann https://orcid.org/0000-0001-5127-3779
Patrick J. Schuler https://orcid.org/0000-0002-1065-8709
Simon Laban https://orcid.org/0000-0001-6732-7137

REFERENCES

1. Bray F, Ferlay J, Soerjomataram I, Siegel RL, Torre LA, Jemal A. Global cancer statistics 2018: GLOBOCAN estimates of incidence and mortality worldwide for 36 cancers in 185 countries. *CA Cancer J Clin*. 2018;68(6):394-424. https://doi.org/10.3322/caac.21492.
2. National Comprehensive Cancer Network (NCCN) Guidelines: Head and Neck Cancers. Version 1.2020. https://www.nccn.org/professionals/physician_gls/pdf/head-and-neck.pdf
3. Burtness B, Harrington KJ, Greil R, et al. Pembrolizumab alone or with chemotherapy versus cetuximab with chemotherapy for recurrent or metastatic squamous cell carcinoma of the head and neck (KEYNOTE-048): a randomised, open-label, phase 3 study. *Lancet*. 2019;394:1915-1928.
4. Cohen EEW, Soulieres D, Le Tourneau C, et al. Pembrolizumab versus methotrexate, docetaxel, or cetuximab for recurrent or metastatic head-and-neck squamous cell carcinoma (KEYNOTE-040): a randomised, open-label, phase 3 study. *Lancet*. 2019;393:156-167.
5. Ferris RL, Blumenschein GJ, Fayette J, et al. Nivolumab for recurrent squamous-cell carcinoma of the head and neck. *New Engl J Med*. 2016;375:1856-1867.
6. Doescher J, Busch CJ, Wollenberg B, et al. Immunotherapy for head and neck cancer: highlights of the 2019 ASCO annual meeting. *HNO*. 2019;67:905-911.
7. Doescher J, Laban S, Schuler PJ, Brunner C, Hoffmann TK. Immunotherapy for head and neck cancers: an update and future perspectives. *Immunotherapy*. 2019;11:561-564.
8. Manukian G, Bar-Ad V, Lu B, Argiris A, Johnson JM. Combining radiation and immune checkpoint blockade in the treatment of head and neck squamous cell carcinoma. *Front Oncol*. 2019;9:122.
9. Mytilineos D, Ezić J, von Witzleben A, et al. Peripheral cytokine levels differ by HPV status and change treatment-dependently in patients with head and neck squamous cell carcinoma. *Int J Mol Sci*. 2020;21 (17):5990. https://doi.org/10.3390/ijms21175990.
10. Jacobs MV, de Roda Husman AM, van den Brule AJ, Snijders PJ, Meijer CJ, Walboomers JM. Group-specific differentiation between high- and low-risk human papillomavirus genotypes by general primer-mediated PCR and two cocktails of oligonucleotide probes. *J Clin Microbiol*. 1995;33:901-905.
11. Borsellino G, Kleinewietfeld M, Di Mitri D, et al. Expression of ecto-nucleotidase CD39 by Foxp3+ Treg cells: hydrolysis of extracellular ATP and immune suppression. *Blood*. 2007;110:1225-1232.
12. Micallef L, Rodgers P. eulerAPE: drawing area-proportional 3-Venn diagrams using ellipses. *PLoS One*. 2014;9:e101717.
13. Watts TH. TNF/TNFR family members in costimulation of T cell responses. *Annu Rev Immunol*. 2005;23:23-68.
14. Qin S, Xu L, Yi M, Yu S, Wu K, Luo S. Novel immune checkpoint targets: moving beyond PD-1 and CTLA-4. *Mol Cancer*. 2019;18:155.
15. Bogdándi EN, Candéias S, Garcia LC, et al. Radiotherapy-induced changes in the systemic immune and inflammation parameters of head and neck cancer patients. *Cancers*. 2019;11(9):1324. https://doi.org/10.3390/cancers11091324.
16. Kimmeyer J, Kurzweg T, Hoffmann TK, et al. Oncologic treatment landscape for head and neck squamous cell carcinoma: treatment infrastructure in German-speaking countries. *HNO*. 2016;64:494-500.
17. Kurzweg T, Kimmeyer J, Knecht R, et al. Curative treatment of head and neck squamous cell carcinoma: organ preservation strategies in clinical routine in German-speaking countries. *HNO*. 2016;64:501-507.
18. Li D, Chen R, Wang YW, Fornace AJ Jr, Li HH. Prior irradiation results in elevated programmed cell death protein 1 (PD-1) in T cells. *Int J Radiat Biol*. 2018;94:488-494.
19. Hecht M, Gostian A, Eckstein M, et al. Single cycle induction treatment with cisplatin/docetaxel plus durvalumab/tremelimumab in stage III-IVB head and neck squamous cell cancer (CHECKRAD-CD8 trial). *Ann Oncol*. 2019;30(suppl_5):v449-v474.

20. Machiels J-PH, Licitra L, Rischin D, et al. KEYNOTE-412: pembrolizumab (pembro) in combination with chemoradiation versus chemoradiation alone in locally advanced head and neck squamous cell carcinoma (LA-HNSCC). *J Clin Oncol*. 2017;35:TPS6090-TPS.

21. Bonomo P, Desideri I, Loi M, et al. Anti PD-L1 DUrvalumab combined with Cetuximab and RadiOtherapy in locally advanced squamous cell carcinoma of the head and neck: a phase I/II study (DUCRO). *Clin Transl Radiat Oncol*. 2018;9:42-47.

22. Yu Y, Lee NY. JAVELIN head and neck 100: a phase III trial of avelumab and chemoradiation for locally advanced head and neck cancer. *Future Oncol*. 2019;15:687-694.

23. Uppaluri R, Lee NY, Westra W, et al. KEYNOTE-689: phase 3 study of adjuvant and neoadjuvant pembrolizumab combined with standard of care (SOC) in patients with resectable, locally advanced head and neck squamous cell carcinoma. *J Clin Oncol*. 2019;37: TPS6090-TPS.

24. Cillo AR, Kurten CHL, Tabib T, et al. Immune landscape of viral- and carcinogen-driven head and neck cancer. *Immunity*. 2020;52: 183-99 e9.

25. Long M, Beckwith K, Do P, et al. Ibrutinib treatment improves T cell number and function in CLL patients. *J Clin Invest*. 2017;127:3052-3064.

26. Chen YL, Lin HW, Chien CL, et al. BTLA blockade enhances cancer therapy by inhibiting IL-6/IL-10-induced CD19(high) B lymphocytes. *J Immunother Cancer*. 2019;7:313.

27. Radvanyi LG, Bernatchez C, Zhang M, et al. Specific lymphocyte subsets predict response to adoptive cell therapy using expanded autologous tumor-infiltrating lymphocytes in metastatic melanoma patients. *Clin Cancer Res*. 2012;18:6758-6770.

28. Turaj AH, Hussain K, Cox KL, et al. Antibody tumor targeting is enhanced by CD27 agonists through myeloid recruitment. *Cancer Cell*. 2017;32:777-91.e6.

29. Trivedi S, Srivastava RM, Concha-Benavente F, et al. Anti-EGFR targeted monoclonal antibody isotype influences antitumor cellular immunity in head and neck cancer patients. *Clin Cancer Res*. 2016;22: 5229-5237.

30. Braig F, Kriegs M, Voigtlaender M, et al. Cetuximab resistance in head and neck cancer is mediated by EGFR-K521 polymorphism. *Cancer Res*. 2017;77:1188-1199.

31. Wolf Y, Anderson AC, Kuchroo VK. TIM3 comes of age as an inhibitory receptor. *Nat Rev Immunol*. 2020;20:173-185.

32. Mohme M, Schliffke S, Maire CL, et al. Immunophenotyping of newly diagnosed and recurrent glioblastoma defines distinct immune exhaustion profiles in peripheral and tumor-infiltrating lymphocytes. *Clin Cancer Res*. 2018;24:4187-4200.

33. Williams P, Basu S, Garcia-Manero G, et al. The distribution of T-cell subsets and the expression of immune checkpoint receptors and ligands in patients with newly diagnosed and relapsed acute myeloid leukemia. *Cancer*. 2019;125:1470-1481.

34. Takenaka MC, Robson S, Quintana FJ. Regulation of the T cell response by CD39. *Trends Immunol*. 2016;37:427-439.

35. Gu J, Ni X, Pan X, et al. Human CD39(hi) regulatory T cells present stronger stability and function under inflammatory conditions. *Cell Mol Immunol*. 2017;14:521-528.

36. Fang F, Yu M, Cavanagh MM, et al. Expression of CD39 on activated T cells impairs their survival in older individuals. *Cell Rep*. 2016;14: 1218-1231.

37. Dwyer KM, Hanidziar D, Putheti P, et al. Expression of CD39 by human peripheral blood CD4+ CD25+ T cells denotes a regulatory memory phenotype. *Am J Transplant*. 2010;10:2410-2420.

38. Duhen T, Duhen R, Montler R, et al. Co-expression of CD39 and CD103 identifies tumor-reactive CD8 T cells in human solid tumors. *Nat Commun*. 2018;9:2724.

39. Kortekaas KE, Santegoets SJ, Sturm G, et al. CD39 identifies the CD4 (+) tumor-specific T-cell population in human cancer. *Cancer Immunol Res*. 2020;8:1311-1321.

40. Allan SE, Crome SQ, Crellin NK, et al. Activation-induced FOXP3 in human T effector cells does not suppress proliferation or cytokine production. *Int Immunol*. 2007;19:345-354.

41. Santegoets SJ, Dijkgraaf EM, Battaglia A, et al. Monitoring regulatory T cells in clinical samples: consensus on an essential marker set and gating strategy for regulatory T cell analysis by flow cytometry. *Cancer Immunol Immunother*. 2015;64:1271-1286.

42. Wild CA, Bergmann C, Fritz G, et al. HMGB1 conveys immunosuppressive characteristics on regulatory and conventional T cells. *Int Immunol*. 2012;24:485-494.

43. Wild CA, Brandau S, Lotfi R, et al. HMGB1 is overexpressed in tumor cells and promotes activity of regulatory T cells in patients with head and neck cancer. *Oral Oncol*. 2012;48:409-416.

44. Giraldo NA, Becht E, Vano Y, et al. Tumor-infiltrating and peripheral blood T-cell immunophenotypes predict early relapse in localized clear cell renal cell carcinoma. *Clin Cancer Res*. 2017;23: 4416-4428.

45. Kovacsovics-Bankowski M, Chisholm L, Vercellini J, et al. Detailed characterization of tumor infiltrating lymphocytes in two distinct human solid malignancies show phenotypic similarities. *J Immunother Cancer*. 2014;2:38.

46. Foulds GA, Vadakekolathu J, Abdel-Fatah TMA, et al. Immunephenotyping and transcriptomic profiling of peripheral blood mononuclear cells from patients with breast cancer: identification of a 3 gene signature which predicts relapse of triple negative breast cancer. *Front Immunol*. 2018;9:2028.

SUPPORTING INFORMATION

Additional supporting information may be found online in the Supporting Information section at the end of this article.